ARMA 13-533

# Coulomb stress change during and after tensile fracture oper geothermal reservoir

Urpi, L.
*GFZ German Research Centre For Geosciences, Potsdam, Germany*
Blöcher, G. and Zimmermann, G..
*GFZ German Research Centre For Geosciences, Potsdam, Germany*



This paper was prepared for presentation at the 47th US Rock Mechanics / Geomechanics Symposium held in San Francisco, CA, USA, 23-26 June 2013.



**ABSTRACT:** Stress shadowing and change in the ratio of shear to normal stress of the rock mass surrounding a newly created tensile fracture are investigated in a typical geothermal reservoir stimulation reservoir scenario. Shearing on plane of weakness near the stimulated volume can be inhibited or promoted by change in poro- and thermo-elastic stress, while pore pressure increase tends to promote failure, via reduction of effective stress, when acting on a failure plane. A numerical model has been used to calculate the coupled poro-elastic response and it has been verified against analytical solution available in literature. The triggering of seismicity, by pore pressure change and stress changes, can be delayed by stress shadowing with respect to the expected occurence triggered by pore pressure diffusion only. Different shut-in schedule may be employed to mitigate unwanted seismicity response to stimulation treatment.

## 1. INTRODUCTION

Enhanced Geothermal System (EGS) and Hot Dry Rock (HDR) geothermal system are characterized by low natural permeability, that must be enhanced to achieve flow rate high enough to achieve the target set for heat extraction and/or power production. Stimulation of the target reservoir with hydraulic fracturing and hydraulic shearing have been performed in various site, with different stress regime and geological setting. Seismic events with maximum magnitude ranging from -3 up to 3 have been recorded in various Enhanced Geothermal System and Hot Dry Rock reservoir stimulation experience, showing distinct time and spatial pattern, involving different processes at different time scale. In this study we focus on the evaluation of poroelastic response of the rock mass to a tensile fracture created injecting cold fluid at pressure high enough to overcome minimum in-situ stress and tensile strength of the rock.

Shearing on plane of weakness near the stimulated volume can be inhibited or promoted by change in poro- and thermo-elastic stress, while pore pressure increase tends to promote failure, via reduction of effective stress, when acting on a failure plane. The occurrence of seismicity, triggered by pore pressure change, can be delayed by stress shadowing due to tensile opening of fracture or even inhibited. Difference in temperature between the injected fluid and the rock mass will induce additional stress perturbation.

Coupling between different processes has been included or excluded according to the relative time scale. The model has no pre-existing plane of weakness and at this stage is useful to determine where seismic events may be triggered due to the Coulomb stress change.

Different tectonic regime has been investigated and the relative influence of pore pressure and thermo-poro-elastic stress changes on in-situ shear and normal stress for arbitrary plane has been evaluated. The fracture data used in the model are based on the stimulation treatment performed in 2007 at the Groß Schönebeck (Germany) EGS test site, where a vertical tensile fracture has been created in a low permeable formation at more than 4000m depth, by injection of 13,170 m³ of fluids and 24.4 tons of quartz sand, with wellhead pressure up to 58.6 MPa and flow rate of 150 L/s in 5 days.

According to this study, different end of stimulation treatment aimed at maintaining fracture open while overpressure dissipate may be effective in mitigate unwanted seismicity.

## 2. POROELASTIC COUPLING

Analytical solutions for stress and pore pressure due to fluid injection into an infinite homogeneous poroelastic medium have been obtained by Rudnicki [1], following Biot classical poroelastic approach.

In a porous elastic media strain and total stress, respectively $\varepsilon$ and $\sigma$, can be expressed via Hooke's law with an additional term accounting for the transfer of stress from the pore space to the rock matrix

$$\sigma_{ij} = \mu(\varepsilon_{ij} + \varepsilon_{ji}) + \lambda\varepsilon_{kk}\delta_{ij} - 2\eta p\delta_{ij} \qquad (1)$$

where $\mu$ and $\lambda$ are the Lamé constants and $\eta$ the poroelastic stress coefficient expressed by $\nu$ the Poisson's ratio and the $\alpha$ Biot-Willis coefficient

$$\eta = \frac{1-2\nu}{2(1-\nu)}\alpha \qquad (2)$$

A second constitutive relation is needed for $\Delta m$, the alteration of fluid (density $\rho_0$) mass content per unit volume of porous solid:

$$\Delta m = 2\eta\rho_0\left[\varepsilon_{kk} + \frac{2\eta}{(\lambda_u - \lambda)}p\right] \qquad (3)$$

denoting with $\lambda_u$ the undrained Lamé modulus.

We can obtain the undrained response due to a sudden change in stress, by setting $\Delta m$ equal to zero and by substituting $\varepsilon_{kk}$ from Eq. (1), obtaining

$$p = -\frac{B}{3}\sigma_{kk} \qquad (4)$$

where $B = (\lambda_u - \lambda)/2\eta(\lambda_u + \frac{2}{3}\mu)$ is Skempton's pore pressure coefficient. Assuming Darcy's law:

$$q = \frac{k_f}{\rho_f g}\nabla p \qquad (5a)$$

valid, with $k_f$ hydraulic conductivity, $\rho_f$ fluid density and considering continuity equation, including an external source an inhomogeneous diffusion equation for pore pressure can be written:

$$\frac{\alpha}{(\lambda + \frac{2}{3}\mu)B}\left[\frac{B}{3}\frac{\partial\sigma_{kk}}{\partial t} + \frac{\partial p}{\partial t}\right] - k_f\nabla^2 p = Q \qquad (5b)$$

Poroelastic coupling strongly affects the solution, since stress change due to displacement like opening/closure of tensile fracture are reflected in the pore pressure distribution. The stress-dependent term can be included in the source term, leading to an inhomogeneous pressure diffusion equation with a time-dependent source/sink term:

$$\frac{\alpha}{(\lambda + \frac{2}{3}\mu)B}\left[\frac{\partial p}{\partial t}\right] - k_f\nabla^2 p = Q(x,t) \qquad (6)$$

## 3. COULOMB FAILURE STRESS

Coulomb criterion predicts initiation of failure on pre-existing planes of weakness when shear stress acting across a certain plane surpasses a critical value $\vec{\tau}_0$

$$|\vec{\tau}_0| = C + \mu\sigma_n \qquad (7)$$

where $C$ is the cohesion of the material (generally assumed very low or absent on plane of shearing), $\mu$ is the coefficient of friction and $\sigma_n$ the normal load acting on the plane [2]. In the presence of pore fluid with pressure p, Eq. (1) must be corrected in accord with the effective stress law yielding

$$|\vec{\tau}_0| = C + \mu(\sigma_n + p) \qquad (8)$$

As a measure of proximity to failure, the Coulomb failure stress $\sigma_c$ can be defined as:

$$\sigma_c = \tau_r + \mu(\sigma_n + p) - C \qquad (9)$$

where $\tau_r$ is the shear stress on the plane in the expected rake (slip) direction.

Negative values of $\sigma_c$ imply that the failure threshold has not yet been reached; zero or positive value imply that the failure threshold has been reached or exceeded.

If C remains constant, then the change in $\sigma_c$ produced on a plane depends on pressure, shear stress and normal stress change

$$\Delta\sigma_c = \Delta\tau_r + \mu(\Delta\sigma_n + \Delta p) \qquad (10)$$

Positive change indicate a stress situation evolving towards failure, while negative change indicates stabilization of the plane.
How in-situ stress distribute in shear and normal stress depends both on tectonic setting and weakness plane orientation.
As a consequence of the effective stress definition, pore pressure increase is generally associated with normal stress reduction, potentially unclamping the plane and promoting shearing. However, reduction of pore pressure can act in opposite direction, due to poro-elastic coupling between pore pressure and local stress.

It has been proven that pore pressure increase for a reservoir located in a normal fault regime cause a negative Coulomb stress change, bringing fault favorably oriented for slipping to stability, while reduction in pore pressure leads to destabilization of rock [3, 4]. Whether induced by poroelastic coupling or by deformation due to fracture opening, stresses that counteract the increase of $\sigma_c$ due to pore pressure increase are identified as stress shadow and they play a role in the occurrence and in the spatial and time pattern shown by microseismic events.

## 4. THERMOELASTIC COUPLING

The heat loss from the cooled fracture with respect to the surrounding rock mass can be approximated through a 1D conductive equation. Representing with $z$ the direction perpendicular to the fracture wall and with $\alpha$ the saturated rock mass thermal diffusivity, the differential equation that has to be solved to obtain the temperature field can be written as:

$$\frac{\partial T}{\partial t} = \alpha \frac{\partial^2 T}{\partial z^2} \tag{10}$$

According to Nowacki [5], we can obtain thermoelastic stress by calculating the termoelastic potential $\phi$ due to a change from initial temperature:

$$\sigma_{ij} = 2\mu\left(\frac{\partial^2 \phi}{\partial x_i \partial x_j} - \frac{1+\nu}{1-\nu}\beta\Delta T\right) \tag{11}$$

where $\Delta T$ is the change from initial temperature and $\beta$ the coefficient of linear expansion coefficient for the rock mass. Vertical stress for a 5 days injection of fluid at 20°C in a reservoir at 150°C are plotted in Fig. 1

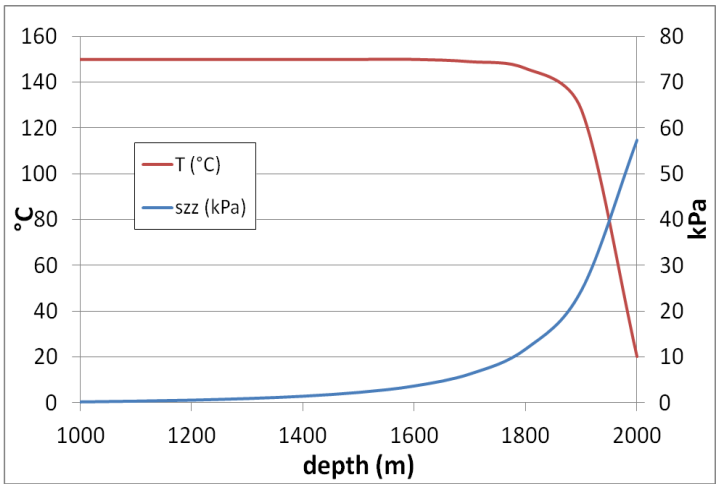


Fig. 1. Tensile stress acting perpendicolar to the fracture (blue) and temperature (red), versus depth for an horizontal fracture at 2000m depth, calculated according to Eq. (11).

The opening on the stimulated fracture plane associated with this temperature change is of the order of some tenth of millimeters, at least two orders of magnitude smaller than the hydraulic opening due to high pressure injection. However, the thermal effect stays longer in place, due to the thermal diffusivity being many order of magnitude smaller than the hydraulic diffusivity.

## 5. FRACTURE INDUCED STRESS AND STRAIN

Injection of fluid in intact rock, at pressure higher than the minimum tectonic stress and the fracture toughness value is necessary to open and propagate a fracture. It is beyond the scope of this study to determine fracture dimensions or to calculate pore pressure needed, we will refer to the results obtained for a stimulation treatment performed in a deep low permeable EGS reservoir in the Northeast German Basin [6]. A total fracture length of 380m and an height of 90 m has been modeled using FRACPRO, with a computed maximum fracture of 2cm. The fracture width is particularly important, to determine the strain and the stresses which the surround rock undergoes.
Viscosity of the fraccing fluid has a strong influence on the fracture size, the PKN analytical model for fracture propagation assumes the following equation for average width:

$$W = 2.52\left[\frac{(1-\nu)Q\mu L}{G}\right]^{1/4} \tag{12}$$

Where $G$ represents Young's modulus, $Q$ the flow rate, $L$ the fracture length. Since viscosity is the parameter that span different orders of magnitudes, depending on the fraccing fluid composition, width is most sensitive to this parameter. Okada provides a complete suite of closed analytical expressions for displacements, strains and tilts due to tensile faults in half-space for finite rectangular source [7].

Approximating our hydraulic fracture as such a source, it is possible to validate the obtained numerical results to quantify stress shadow. The distribution in space of change in stress is as important as the magnitude, because of the different relative importance of stress distribution between shear and normal. The analytical solution provided take into account free surface and the elastic bi-harmonic potential from which displacement are derived goes to zero at distance from the fracture. Okada solution does not provide undrained response for a saturated rock, but the pressure response can be obtained with Eq. (4) for singular values or solving Eq. (6) with appropriate boundary conditions. In Fig. 2 it is possible to see an example of stress distribution for an

horizontal fracture, 380 m length 90 m width and at 2000 m depth, created in a thrust faulting tectonic regime. The fracture centre coordinates are (0,0,-2000), stresses are $\sigma_1 = \sigma_H = 80$MPa, $\sigma_3 = \sigma_v = 48$ Mpa, formation pressure 26 MPa) and the elastic parameter for the analytical solution and for the numerical model are noted in Table 1, in the successive section. The stress change pattern obtained for the horizontal fracture is visible in Fig. 2-3-4. This pattern will not be different for the other tectonic settings, because the fracture:

- is deep enough not to be influenced by the free surface
- will be oriented according to the minimum and maximum stress orientation.

The pattern for the other tectonic settings (normal faulting and strike-slip) will be simply the rotation of the thrust fault pattern here depicted.

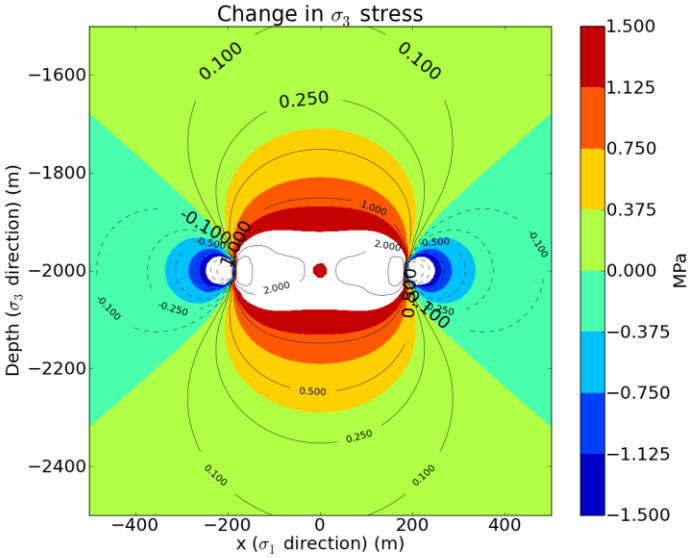


Fig. 2. Change in vertical stress on the σ1−σ3 plane. In this setting red zones are subject to compressive stress, blue zones to tensile.

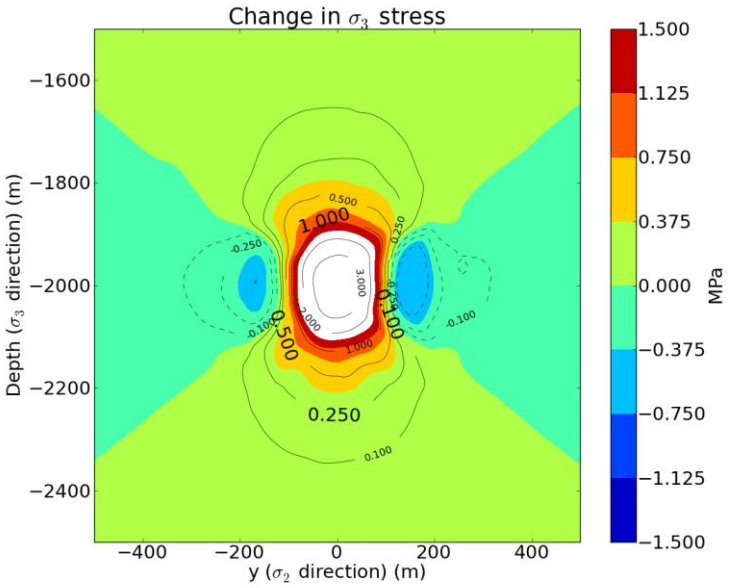


Fig. 3 Change in vertical stress on the σ2−σ3 plane. Red zones are subject to compressive stress, blue zones to tensile.

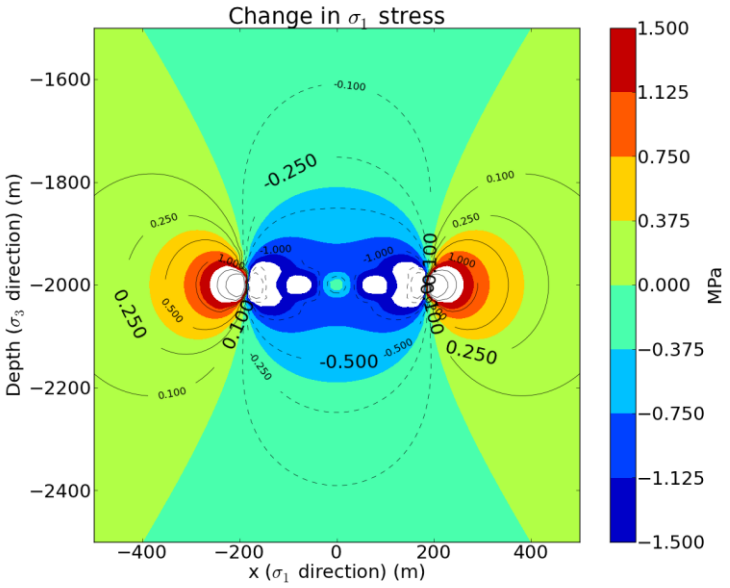


Fig. 4 Change in horizontal (maximum) stress on the σ1−σ3 plane.

## 6. NUMERICAL MODEL

A standard Galerkin finite element spatial discretization with time discretization following a generalized first order has been used [8]. The model is a cube of 5 km size, while the fracture is introduced as a displacement time-dependent boundary condition. Evaluation of fracture status (close/open) and of the fluid pressure in the fracture are calculated

externally and given in the model as boundary condition. A set of coupled linear equations is be solved for the primary variables, liquid pressure $p$ and solid deformation $u$.
For the time scale involved in the stimulation treatment (hours to days) the temperature perturbation is not influencing at a great distance, but there is an effect in the immediate surroundings of the fracture. The equation system is solved with a one-step monolithic algorithm. Properties of the rock mass and of the fluid are summed up here.

Table 1: Solid properties

| Properties | Symbol | Unit | Value |
|---|---|---|---|
| Density | ρ | kg/m³ | 2600 |
| Young's m. | E | GPa | 10 |
| Poisson ratio | ν | ---- | 0.3 |
| Permeability | κ | m² | $10^{-14}$ |
| Porosity | φ | % | 8 |
| Biot-Willis | α | ---- | 0.8 |
| Thermal expansion | $\beta$ | $K^{-1}$ | $6.0\ 10^{-6}$ |

Table 2: Fluid properties

| Properties | Symbol | Unit | Value |
|---|---|---|---|
| Density | ρ | kg/m³ | 1000 |
| Viscosity | η | Pa s | $10^{-3}$ |
| Spec.heat capacity | λ | J/(kg K) | 4.181 |

The numerical model reproduces correctly the analytical solution and this can be verified by direct comparison of a stress profile perpendicular to the fracture, looking at the numbers there are some difference at the low pressure values, but it should be possible to correct by having a finer mesh at distance from the fracture.

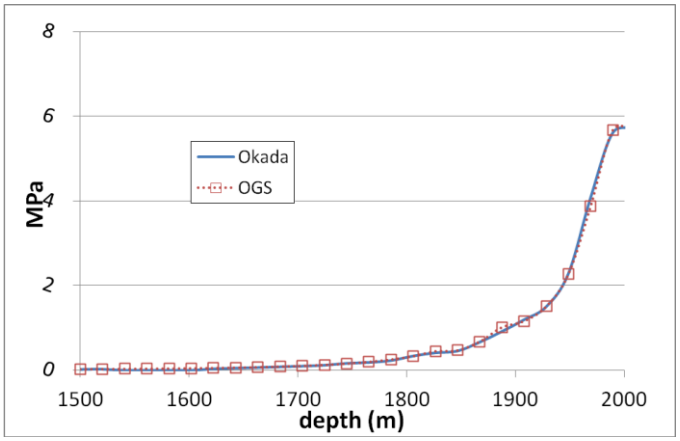


Fig. 5. Analytical and numerical Comparison for stress trend in direction perpendicular to the fracture.

The numerical solution apart from being in agreement with Okada model, and in accordance con Eq. (4) it reproduces the undrained response, with an increase of pore pressure around the fracture as visible in Fig. 6

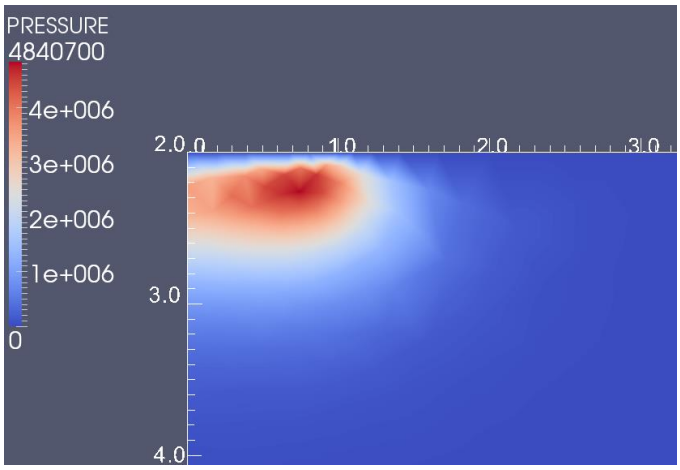


Fig. 6. Undrained response and initiation of pore pressure propagation.

A refined time dependent boundary condition is needed to determine correctly which part of the fracture wall is actually under effect of high pore pressure from the stimulation treatment. At the moment the fracture opening criteria is rigidly depending on external data, without any update from the elastic response of the reservoir. Not reported here, but calculated in the model, displacement and strain are computed and can be helpful to monitor the fracture propagation, while temperature change are almost negligible, because of low permeability in the rock matrix heat conduction is the dominant process and it is happening on a time scale much larger than pore pressure diffuson. Due to this fact, its influence on stress perturbation is very localized, although transport of cold fluid through a natural system of fracture/joints may increase the importance of the thermoelastic stresses.

## 7. DISCUSSION AND CONCLUSIONS

Considering the three dimensional perturbation of stresses and the variability of shear to normal stress-ratio, depending on the orientation of planes of weakness that may be present in the surrounding of the fracture, the stress perturbation arising from the stimulation treatment shows some distinct features.
Due to stress shadow, the planes parallel to the fracture are generally stabilized during the fracture propagation and as long as the fracture is open, we have stress perturbation of the order of 0.1 MPa in a range as far as the fracture length. Thermo-elastic perturbation for this temperature range seems to play a negligible role, although potential for creation of thermal fracture has not been evaluated. Irrespective of the tectonic regime, on the maximum stress axis we have a strong negative Coulomb stress change. Combined reduction of normal stress and increase of shearing stress can increase the occurrence of seismic events in the direction of fracture propagation. This may lead to over-estimation in

deriving the stimulated volume from micro-seismic monitoring and/or can connect hydraulically the tensile fracture with structure that carry away fraccing fluid.

In Fig. (2) and (4) it is possible to see how the stabilizing effect of the open fracture is stronger in the direction perpendicolar to the fracture wall. Since this is the direction where the overpressure from the stimulation is released, it is worthwhile to optimize the stimulation strategy to delay as much as possible the closure of the fracture. It is worthwhile to note that for a critical stressed situation, even a change in stress of less than 1 MPa can make a difference,as visible in Fig. 7.

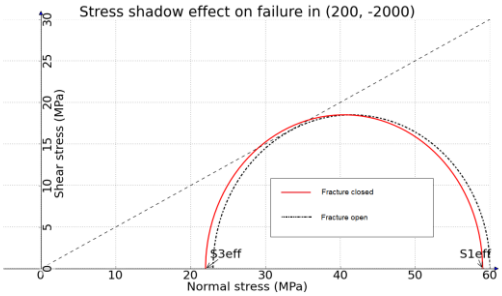


Fig. 7. Stress state immediately before and after hydro-fracture closure, tectonic regime as in Fig.(5)

Since the stress shadow due to tensile opening is in place only until the fracture is open, it means that in low permeable formation the fracture closure will happen sometime after the stop of the injection. If this is the case, a correct shut-in procedure should be asseessed not only on the base of pore pressure diffusion but also on the stress change induced. Therefore, acknowledged that the main trigger for seismicity during fluid injection is the pore pressure change, the poroelastic coupling and stress shadow may be an useful tool in mitigating the happening of unwanted seismicity.

## 8. ACKNOWLEDGMENTS

The authors would like to thank the International Energy Agency/Geothermal Implementing Agreement and the US Department of Energy for their support of this paper which we trust encourages international cooperation on topics being pursued by Annex VII, Advanced Geothermal Drilling and Logging Technologies.

## 9. REFERENCES

1. Rudnicki, J. W. 1986. Fluid mass sources and point forces in linear elastic diffusive solids. *Mechanics of Materials*, 5: 383–393.

2. Jaeger, J.C., N.G.W. Cook and R.W. Zimmerman. 2007. *Fundamentals of rock mechanics*. 4 th ed. Wiley-Blackwell Publishing, Oxford, 98-122p.

3. Hillis, R., 2000. Pore pressure/stress coupling and its implications for seismicity. *Exploration Geophysics*, 31: 448-454..

4. Chen, Q., and A. Nur. 1992. Pore fluid pressure effects in anisotropic rocks: mechanism of induced seismicity and weak faults. *Pure and Applied Geophysics*, 139: 463-479

5. Nowacki, W. 1986. Thermoelasticity. 2nd ed. Pergamon Press. 44-80.

6. Zimmermann, G., I. Moeck and G. Blöcher. 2010. Cyclic waterfrac stimulation to develop an Enhanced Geothermal System (EGS)—Conceptual design and experimental results. *Geothermics* 39:70-77,

7. Okada, Y. 1992. Internal deformation due to shear and tensile faults in a half-space, *Bull. Seismol. Soc. Am.*, 82: 1018–1040.

8. Kolditz O. , S. Bauer, L. Bilke, N. Böttcher, J. O. Delfs, T. Fischer, U. J. Görke, T. Kalbacher, G. Kosakowski, C. I. McDermott, C. H. Park, F. Radu, K. Rink, H. Shao, H. B. Shao, F. Sun, Y. Y. Sun, A. K. Singh, J. Taron, M. Walther, W. Wang, N. Watanabe, Y. Wu, M. Xie, W. Xu, B. Zehner. 2012. OpenGeoSys: an open-source initiative for numerical simulation of thermo-hydro-mechanical/chemical (THM/C) processes in porous media. *Environmental Earth Sciences*, 67: 589-599